Regular Article

PHYSICAL CHEMISTRY RESEARCH
Published by the
Iranian Chemical Society
www.physchemres.org
info@physchemres.org

Phys. Chem. Res., Vol. 11, No. 4, 735-745, December 2023
DOI: 10.22036/pcr.2022.356470.2168

Volumetric Properties of Nanofluids by a Perturbed Hard-sphere Chain Equation of State

F. Mozaffari[a] and Z. Sharafi[b,*]

[a]*Department of Chemistry, Faculty of Nano and Bio Science and Technology, Persian Gulf University, Bushehr, 75168, Iran*
[b]*Department of Chemistry, Marvdasht Branch, Islamic Azad University, Marvdasht, Iran*
(Received 16 August 2022, Accepted 2 November 2022)

A perturbed hard-sphere chain equation of state (PHSC) is employed to predict the volumetric properties of some nanofluids containing Co_3O_4 in ethylene glycol (EG), SnO_2 in EG, TiO_2-anatase (-A) in EG, TiO_2-rutile (-R) in EG, Al_2O_3 in EG/H_2O, Sb_2O_5-SnO_2 in EG/H_2O, ZnO in polyethylene glycol (PEG)/H_2O and CuO in H_2O. Two temperature-dependent parameters in the proposed EoS were expressed in terms of molecular scaling constants σ; effective hard-sphere diameter, and ε; non-bonded interaction energy. The mentioned scaling constants were correlated with melting temperatures and densities which shows the rationality of them. It is also indicated in this study without knowledge of potential energy function can able to illustrate the volumetric properties of nanofluids. Comparisons between the calculated liquid densities and the experimental values over the temperature range from 273.15 to 363.15 K and the pressure range from 0.1 to 45 MPa show that the average absolute deviation is 1.49%.

Keywords: Equation of state, Modeling, Nanofluids, Density

INTRODUCTION

A nanofluid is defined as a colloidal system of solid particles, fibers, rods, or tubes with nanometer size (denoted as nanoparticle) that is distributed in a fluid (denoted as base fluid). One of the advantages of using nanofluids is that they can be reduced the size of required heat exchangers and ultimately energy and material consumption is reduced [1]. Nowadays, environmental problems and damaging effects created by growing fossil fuel consumption that are vanishing reserves are yet one of the important problems to be right away dealt [2]. Economically, water and ethylene glycol are widely used as base fluids. Due to the low thermal conductivity of these fluids, their use as heat transfer fluids in limited spaces such as electronic equipment and concentrated solar radiation converters is very limited. According to new findings suspending solid nanoparticles in liquids significantly increases effective thermal conductivity [3], but the suspension of millimeter or micrometer particles increases the Sedimentation speed and creates a layer on the surface, and decreasing the fluid heat transfer capacity [4]. When the size of the particles is large, it can lead to clogging of the flow channels, especially for narrow cooling channels and the fluid pressure drop increases significantly [4]. Due to the high heat transfer ability of metal and metal oxide nanofluids, extensive investigations on these fluids in order to use them in cooling electronic appliances, solar and automotive have been done. Hafiz M. A. *et al*. [5] introduced an effective method to increase the efficiency of heat transfer in a car radiator using water-based ZnO nanofluids. The effect of temperature and particle size along with nanoparticles concentration on the effective thermal conductivity of alumina/water and copper oxide/water nanofluids were investigated by Mintsa *et al.* [6]. Extensive investigations have been done by Chandrasekar et al [7] both experimentally and theoretically to determine the effective thermal conductivity and viscosity of Al_2O_3/H_2O of nanofluids. Asleshirin *et al*. [8] measured the effect of shape

*Corresponding author. E-mail: zsharafi@miau.ac.ir

alumina nanoparticles on the thermophysical properties of 1-hexyl-3-methylimidazolium hexafluorophosphate as ionic base fluids (green solvents) such as density, viscosity, thermal conductivity, and heat capacity at different concentration of nanoparticles and temperatures. According to a theoretical model presented by Ren *et al*. [9], the increase in the effective thermal conductivity of nanofluids due to the effects of the interfacial layer and particle motion was considered. The experimental results obtained by Chavan *et al*. [10] clearly show that the viscosity of nanofluids, increases with increasing in particle volume concentration and decreases with increasing in temperature of nanofluids. In order to predict the heat transfer behavior of nanofluids, their thermophysical properties are quite essential. For these advantages, nanofluids have attracted much attention and have been widely used in many engineering applications such as nuclear reactors, energy efficiency enhancers, food industry, air conditioning systems, refrigeration, heating, and biomedicine [11-21]. Due to the high thermal efficiency of nanofluids compared to water in heating and cooling processes, these fluids can be used instead of water in heat exchangers. Therefore, in most cases, the volume of water consumption can be reduced and also the problems related to the production of large industrial wastes such as the oil industry and especially petrochemical industries can be solved [20]. Density values of nanofluids are necessary to evaluate fluid dynamics and heat transfer efficiency [22-24]. Vajjha *et al*. [25] measured the experimental density of three different nanofluids containing aluminum oxide (Al_2O_3), antimony-tin oxide (Sb_2O_5:SnO_2), and zinc oxide (ZnO) nanoparticles in a base fluid of 60:40 ethylene glycol/water by mass. Despite of significance of density in heat transfer calculations, less attention has been dedicated to that. However, experimental measurement of nanofluids density has restrictions on preparing monodisperse suspensions, homogeneity of its solution, and difficulty in measuring the size of particle. Whereas the experimental density of nanofluids is scarce, theoretical methods such as equations of state (EoS) and $P\rho T$ correlations seem to be beneficial. Pak and Cho [26] introduced an equation for density of nanofluids as follows:

$$\rho_{nf} = \rho_{np}\varphi + \rho_{bf}(1-\varphi) \quad (1)$$

where, ρ_{bf}, ρ_{nf}, and ρ_{np} are the density of the base fluid, nanofluid, and nanoparticles respectively and φ is the particle volume concentration. Pak and Cho performed this experiment at only one temperature (25 °C) for γ- Al_2O_3 and TiO_2 nanofluids up to 4.5% volume concentration to verify Eq. (1). However, the Pak-Cho equation requires knowing the correct of the base fluid and nanoparticle densities to the determined nanofluids density and poor accuracy in determining the density of dry powder, ρ_{np}, restricts the applicability of the Pak-Cho equation.

Equation of states and their correlations [27-30] are widely used to predict the thermodynamic properties of the liquid phase for pure and fluid mixtures. Recently, we have applied a statistical-mechanical method to calculate the volumetric properties of ionic liquids and mixture of liquid refrigerants [31-33].

In this paper, we investigate the applicability of perturbed hard sphere chain (PHSC) EoS to predict the volumetric properties of nanofluids. The results showed that PHSC EoS by using crossed interaction parameters between base fluid and nanoparticle can suitably model thermophysical properties of extremely nonsimple fluids.

THEORY

Equation of State for Pure Base Fluid

Song *et al.* and Eslami [34,35] proposed PHSC EoS based on the statistical-mechanical perturbation theory. In the field of PHSC theory, a chain molecule as a chain of freely connected tangent of hard bodies is assumed. The PHSC equation of state uses a hard-sphere-chain reference system plus a van der Waals attractive perturbation:

$$\frac{P}{\rho kT} = 1 + r^2 b(T)\rho g(d^+) - (r-1)[g(d^+) - 1] - \frac{r^2 a(T)\rho}{kT} \quad (2)$$

where P is the pressure, ρ is the number (molar) density, kT is the thermal energy per one molecule, r is the number of segments, $b(T)$ is the van der Waals c per segment or the second virial coefficient of non-bonded hard spheres, d is the hard sphere diameter, $g(d^+)$ is the pair radial distribution function of hard spheres at contact, $a(T)$ reflect the attractive forces between two non-bonded segments. We need a

mathematical expression for $g(d^+)$ to utilize this equation. Carnahan and Starling [36] proposed an analytical expression for $g(d^+)$ as:

$$g(d^+) = \frac{1-\eta/2}{(1-\eta)^3} \tag{3}$$

where η is the packing fraction and defined as:

$$\eta = \frac{rb(T)\rho}{4} \tag{4}$$

Song *et al.* [34] defined *a* (*T*) and *b*(*T*) in terms of pair potential, but they have shown that *a*(*T*) and *b*(*T*) are not sensitive to details of potential. However, for most physical systems especially nanofluids, where the interaction between base fluid and nanoparticles depends on different factors, is rarely identified. Since the pair potential can be defined in terms ε (the depth of the minimum in the pair potential) and σ (the separation distance at minimum of pair potential), then *a*(*T*) and *b*(*T*) can be scaled by these terms and they are given as:

$$a(T) = \frac{2\pi}{3}\sigma^3 \varepsilon F_a(^{kT}/_{\varepsilon}) \tag{5}$$

and

$$b(T) = \frac{2\pi}{3}\sigma^3 F_b\left(^{kT}/_{\varepsilon}\right) \tag{6}$$

where F_a and F_b are universal functions of reduced temperature $\left(^{kT}/_{\varepsilon}\right)$, which are written as:

$$F_a\left(^{kT}/_{\varepsilon}\right) = \alpha_1 + \alpha_2 e^{-\alpha_3(^{kT}/_{\varepsilon})} \tag{7}$$

$$F_b\left(^{kT}/_{\varepsilon}\right) = \beta_1 e^{-\beta_2(^{kT}/_{\varepsilon})} + (1-\beta_1)[1 - e^{-\beta_3(^{kT}/_{\varepsilon})^{-1/4}}] \tag{8}$$

where α_1, α_2, α_3, β_1, β_2 and β_3 are 0.7170, 1.9003, 0.5152, 0.5849, 0.4772, and 1.0669, respectively.

Extension of the PHSC EoS to Nanofluids

The present PHSC EoS can be generalized to mixtures of any number of components [37,38] as:

$$\frac{P}{\rho kT} = 1 + \rho\sum_{ij}^{m} x_i x_j r_i r_j b_{ij} g_{ij}(d_{ij}^+) - \sum_{i}^{m} x_i (r_i - 1) \times [g_{ii}(d_{ii}^+) - 1] - \frac{\rho}{kT}\sum_{ij}^{m} x_i x_j r_i r_j a_{ij} \tag{9}$$

where x_i and x_j are mole fractions of components *i* and *j*, respectively, r_i is the number of segments for the *i*-th component, and $g_{ij}\left(d_{ij}^+\right)$ is the pair radial distribution function of hard sphere mixtures at contact. Like Eq. (2) the first three terms in Eq. (9) represent the reference equation of state for hard-sphere-chain mixtures and the last term is a van der Waals-type perturbation for attractive forces. The temperature-dependent parameters a_{ij} (reflecting attractive forces between two unlike segments) and b_{ij} (second cross virial coefficient of hard-sphere mixtures) can be specified by extending Eqs. (5) and (6) to mixtures as:

$$a_{ij}(T) = \frac{2\pi}{3}\sigma_{ij}^3 \varepsilon_{ij} F_{ij}\left(\frac{kT}{\varepsilon_{ij}}\right) \tag{10}$$

and

$$b_{ij}(T) = \frac{1}{8}(b_i^{\frac{1}{3}} + b_j^{\frac{1}{3}})^3 \tag{11}$$

where, σ_{ij} and ε_{ij} can be generated by suitable mixing rules:

$$\varepsilon_{ij} = \sqrt{\varepsilon_{ii}\varepsilon_{jj}}\,(1 - k_{ij}) \tag{12}$$

$$\sigma_{ij} = \frac{\sigma_{ii} + \sigma_{jj}}{2} \tag{13}$$

where, k_{ij} is a binary parameter for measuring the interaction between mixture components.

$F_{ij}(T)$ is a geometrical mean of $F_a(^{kT}/_{\varepsilon})$ for pure components *i* and *j*:

$$F_{ij}(T) = \sqrt{F_a(\frac{kT}{\varepsilon_{ii}})F_a(\frac{kT}{\varepsilon_{jj}})} \tag{14}$$

The well-known expression for $g_{ij}\left(d_{ij}^+\right)$ which demonstrate the pair radial distribution function of hard sphere mixtures is the Mansoori-Carnahan-Starling [39] equation:

$$g_{ij}\left(\eta, \xi_{ij}\right) = \frac{1}{1-\eta} + \frac{3}{2}\frac{\xi_{ij}}{(1-\eta)^2} + \frac{1}{2}\frac{{\xi_{ij}}^2}{(1-\eta)^3} \tag{15}$$

Where η is the packing fraction:

$$\eta = \frac{\rho}{4}\sum_i^m x_i\, r_i b_i \quad (16)$$

$$\xi_{ij} = (\frac{b_i b_j}{b_{ij}})^{1/3}\frac{\rho}{4}\sum_k^m x_k r_k b_k^{2/3} \quad (17)$$

RESULTS AND DISCUSSION

The proposed EoS has been utilized to calculate the volumetric properties of nanofluids. The parameters, ε, σ, and *r* for base fluids were tuned with experimental $P\rho T$ data which were taken from the literature [40-42] and are given in Table 1. These parameters for nanoparticles were adjusted by densities of compacted nanopowder [43] over the desired temperature range.

Three molecular parameters ε, σ, and *r*, along with melting temperature, T_m and density of the intended nanoparticle have been given in Table 2.

We investigate the correlations of ε with melting temperature in Fig. S1 (Supporting Information: SI) and σ with density in Fig. S2, to indicate the reasonability of obtaining molecular parameters for nanoparticles.

In the next step, we applied mixture version of PHSC EoS for binary base fluids, including ethylene glycol (EG) + water and polyethylene glycol (PEG) + water. It should be noted that in the present EoS a binary interaction parameter, k_{ij} is added to compute the crossed attractive parameter for realization the measure of interaction between base fluid-base fluid (k_{12}) and nanoparticle-base fluid (k_{np-}) molecules. The temperature and pressure ranges, the mole fraction of water in binary mixture, the number of

Table 1. The Molecular Scaling Constants of Intended Based Fluids to be Used in Eqs. ((2)-(8))

Pure base fluid	ε/k_B	σ (nm)	r	ΔT (K)	ΔP (MPa)	NP[a]	AAD (%)[b]	Ref.
EG	432.8	0.319	4.06	283.15-343.15	0.1-45	15	0.34	[40]
PEG	429.4	0.59	4.09	298.15-323.15	0.1	6	0.04	[41]
Water	613.0	0.21	4.91	280.00-380.00	0.1-50.1	120	0.65	[42]

[a]NP represents the number of data points examined. [b] $AAD = 100/NP\sum_{i=1}^{NP}\left|\rho_i^{EXP.} - \rho_i^{Calc.}\right|/\rho_i^{EXP.}$.

Table 2. The Molecular Scaling Constants of Intended Nanoparticles to be Used in Eqs. ((2)-(8))

Nanoparticle	ε/k_B	σ (nm)	r	AD^a $(\frac{g}{cm^3})$	D^b $(\frac{g}{cm^3})$	${T_m}^c$ (K)
Co_3O_4	1398.0	0.25997	4.49	6.10	6.11	895
SnO_2	2593.4	0.31600	2.07	6.94	6.95	1630
TiO_2(-A)	2893.0	0.31100	2.16	3.90	3.90	1843
TiO_2(-R)	2992.7	0.31099	2.00	4.18	4.23	1870
ZnO	3092.2	0.28200	2.07	5.59	5.60	1975
Al_2O_3	3304.3	0.34300	2.10	3.90	3.90	2040
Sb_2O_5-SnO_2	2497.21	0.21000	20.49	6.79	6.8	-
CuO	1798.6	0.26199	2.08	6.30	6.31	1201

[a]AD indicates the average density of nanoparticles reproduced from PHSC EoS. [b]D indicates the density of nanoparticles obtained from the literature [43]. [c]T_m indicates the melting temperature of nanoparticles obtained from literature [43].

examined data points of comparison, the binary parameter, and the average absolute deviation percent (AAD%) of the calculated densities of these binary mixtures from experimental values [41,44] from the PHSC EoS are given in Table 3.

As the studied nanofluids contained nanoparticles in pure or binary base fluids, Eqs. ((9)-(17)) are applied for two and three-component mixtures. We have used PHSC EoS to predict the volumetric properties of nine nanofluids containing Co_3O_4 in EG, SnO_2 in EG, TiO_2-anatase (-A) in EG, TiO_2-rutile (-R) in EG, ZnO in EG/H_2O, Al_2O_3 in EG/H_2O, Sb_2O_5-SnO_2 in EG/H_2O, ZnO in PEG/H_2O and CuO in H_2O. The accuracy of predicted results is examined by comparing with experimental data [40,41,44-48] over a wide range of pressures, temperatures, and mole fractions. The number of examined data points, the ranges of temperature, pressure, and mole fraction of nanoparticle in nanofluid and the average absolute deviation percent (AAD%) of the calculated densities for nanofluids from literature values [40,41,44-48] *via* the PHSC EoS are given in Table 4.

Table 5 shows the maximum and minimum deviation percent of calculated densities of Co_3O_4/EG, TiO_2 (-A)/EG, and SnO_2/EG nanofluids in different temperatures and a pressure range of 0.1 to 45.0 MPa from experimental data [40,45,48] using PHSC EoS. As Table 5 shows, the results are in good agreement with the experimental literature data.

Table 3. The Average Absolute Deviation Percent of Predicted Densities of Studied Mixed Base Fluids Using the Proposed PHSC EoS from Literature

Mixed base fluid	ΔT (K)	ΔP (MPa)	Δx_{water}	NP	k_{12}	AAD (%)	Ref.
EG + water	278.15-363.15	0.1-45	0.755-0.755	55	-0.15	1.06	[44]
PEG + water	298.15-323.15	0.1	0.108-0.981	78	0.196	1.99	[41]

Table 4. The Average Absolute Deviation Percent of Predicted Densities of Studied Nanofluids Using the Proposed PHSC EoS from Literature

Nanofluid	ΔT (K)	ΔP (MPa)	Δx_{np}	NP	k_{np-bf}	AAD (%)	Ref.
Co_3O_4/EG	283-323	0.1-45	0.008-0.042	200	-0.016	1.86	[45]
SnO_2/EG	283-323	0.1-45	0.004-0.020	200	-3.63	1.75	[48]
TiO_2(-A)/EG	283-343	0.1-45	0.014-0.039	25	-1.019	1.47	[40]
TiO_2(-R)/EG	283-343	0.1-45	0.014-0.039	30	-1.308	1.82	[40]
ZnO/EG+H_2O	278-363	0.1-45	0.009-0.038	165	0.368[a]	0.96	[44]
	273-323	0.1	0.021-0.041	36	-0.141[b]	2.34	[25]
Al_2O_3/EG+H_2O	273-323	0.1	0.012-0.107	36	0.561	0.66	[25]
Sb_2O_5-SnO_2/EG+H_2O	273-323	0.1	0.005-0.029	30	0.649	0.50	[25]
CuO/H_2O	283-323	0.1-45	0.004-0.020	200	-5.619	1.77	[46]
ZnO/PEG+H_2O	293-318	0.1	9E-5-0.016	45	2.300	1.78	[47]
Overall				967		1.49	

[a]This value was obtained for ZnO nanoparticle with the average particle size equal to 29 nm in nanofluid. [b]This value was obtained for ZnO nanoparticle with the average particle size equal to 70 nm.

Table 5. The Absolute Maximum and Minimum Deviation Percent of Predicted Densities of Studied Nanofluids Using the Proposed PHSC EoS from Literature

Nanofluid	P (MPa)	$\lvert Maximum\ Dev(\%)\rvert$	$\lvert Minimum\ Dev(\%)\rvert$	Ref.
Co_3O_4/EG	0.1	3.48	0.08	[45]
	1.0	3.49	0.01	[45]
	5.0	3.28	0.03	[45]
	10.0	3.34	0.05	[45]
	20.0	3.47	0.09	[45]
	30.0	3.3	0.04	[45]
	40.0	3.4	0.13	[45]
	45.0	3.45	0.08	[45]
SnO_2/EG	0.1	3.29	0.07	[48]
	1.0	3.31	0.09	[48]
	5.0	3.37	0.17	[48]
	10.0	3.45	0.12	[48]
	20.0	3.59	0.04	[48]
	30.0	3.41	0.19	[48]
	40.0	3.22	0.02	[48]
	45.0	3.45	0.08	[45]
TiO_2(-A)/EG	0.1	2.39	0.33	[40]
	1.0	2.41	0.36	[40]
	20.0	2.68	0.53	[40]
	40.0	2.96	0.12	[40]
	45.0	3.03	0.0	[40]

Also, Table 6 indicates the maximum and minimum deviation percent of the calculated liquid densities of ZnO/EG+H_2O, Al_2O_3/EG+H_2O, Sb_2O_5-SnO_2/EG+H_2O and ZnO/PEG+H_2O in different temperature and a pressure range 0.1 to 45.0 MPa from the literature [44,25,47] using the proposed EoS. As obviously indicated in Tables 5 and 6, the predicted densities from the PHSC EoS were in good agreement with the literature data.

The values of deviation can specify that the calculated values are more or less close to the experimental data. Therefore, it can be claimed that the PHSC EoS can predict the experimental density of nanofluids with good accuracy according to the obtained results were given in Table 4. The obtained results which were given in Table 4 show a good capability of the PHSC EoS to calculate the molar density of nanofluids.

The calculated density of nanofluid versus the experimental density from the proposed EoS is plotted as shown in Fig. 1. This figure shows that the PHSC EoS performs excellently in comparison with experimental data for nanofluids containing Co_3O_4, SnO_2, TiO_2-A, TiO_2-R, ZnO, Al_2O_3, Sb_2O_5-SnO_2 as nanoparticles dispersed in EG and EG + water as base fluids in different temperatures, pressures, and mole fractions.

As Fig. 1 indicates, the calculated densities are well distributed along the diagonal, therefore, the results show that the present EoS is capable of predicting the densities of various nanofluids over a broad range of temperatures, pressures, and mole fractions.

Table 6. The Absolute Maximum and Minimum Deviation Percent of Predicted Densities of Studied Nanofluids Using the Proposed PHSC EoS from Literature

Nanofluid	$P(MPa)$	|Maximum $Dev(\%)$|	|Minimum $Dev(\%)$|	Ref.
ZnO/EG+H_2O	0.1	2.53	0.04	[44]
	1.0	2.50	0.04	[44]
	5.0	2.33	0.08	[44]
	10.0	2.14	0.25	[44]
	15.0	1.96	0.18	[44]
	20.0	1.70	0.00	[44]
	25.0	1.59	0.00	[44]
	30.0	1.67	0.13	[44]
	35.0	1.82	0.27	[44]
	40.0	1.95	0.29	[44]
	45.0	2.09	0.13	[44]
Al_2O_3/EG+H_2O	0.1	1.81	0.04	[25]
Sb_2O_5-SnO_2/EG+H_2O	0.1	2.0	0.08	[25]
ZnO/PEG+H_2O	0.1	1.89	0.01	[47]

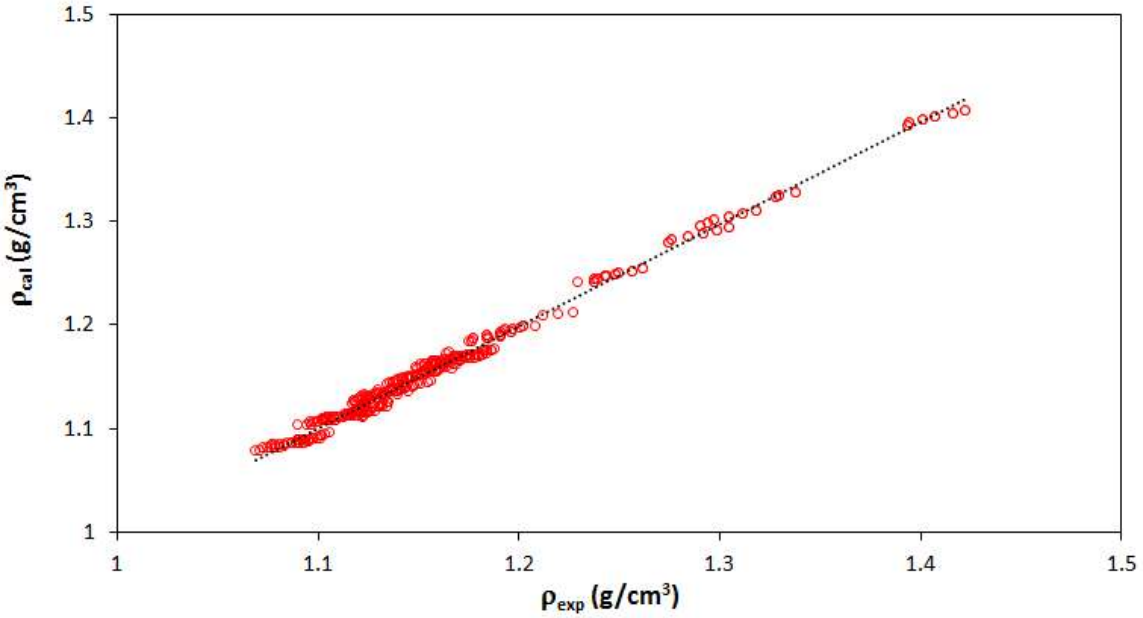

Fig. 1. The predicted densities by the present equation of state for nanofluids containing Co_3O_4, SnO_2, TiO_2-A, TiO_2-R, ZnO, Al_2O_3, Sb_2O_5-SnO_2 as nanoparticles dispersed in EG and EG + water as base fluids at various temperatures, pressures, and mole fractions compared to the experimental data [40,41,44-48].

CONCLUSIONS

In this research, the PHSC EoS was utilized to model the volumetric properties of EG, PEG, water, PEG + water, and EG + water-based nanofluids at different nanoparticle concentrations. In the first step, the estimation of pure component parameters including base fluids and nanoparticles is done, and then, PHSC EoS is extended to mixed base fluids and nanofluids by using binary interaction parameters. Also, this work indicated that without knowledge of potential energy function can able to illustrate the *PVT* properties of nanofluids. Here, we have shown that the adjusting of molecular parameters, ε, σ, and *r* with experimental data provided us an excellent opportunity to scale the temperature-dependent parameters of PHSC EoS. It should be noted that our obtained results accord well with the experimental data. The overall average absolute deviation of calculated densities from literature values is found to be 1.49%.

ACKNOWLEDGEMENTS

We thank the research Committee of Persian Gulf University and Islamic Azad University, Marvdasht Branch for supporting this project.

Nomenclature and Units

b (T): van der Waals covolume of nonbonded hard spheres (m^3)
T: Absolute temperature (K)
P: Pressure (Pa)
k_B: Boltzmann's constant (J K^{-1})
M_w: Molecular weight (g mol^{-1})
a (T): Attractive forces between two nonbonded segments (J m^{-3}):
α_1- α_3: Coefficients that used in Eq. (7)
$\beta_1 - \beta_3$: Coefficients that used in Eq. (8)
F_a and F_b: Universal functions
N_A: Avogadro's number
x: Mole fraction
d: Hard sphere diameter (nm)
$g(d^+)$: Pair radial distribution function of hard spheres at contact
k_{12}: Binary interaction parameters between base fluid-base fluid molecules
k_{nf-bf}: Binary interaction parameters between nanoparticle-base fluid molecules

Greek Letters

σ: Effective hard-sphere diameter (nm)
ε: Non-bonded interaction energy parameter (J)
η: Packing fraction
ρ: Number (molar) density (mol m^{-3})
φ: Particle volume concentration

Superscripts

Calc: Calculated
Exp: Experimental

Subscripts

EoS: Equation of state
bf: Base fluid
np: Nanoparticle

REFERENCES

[1] Gupta, K. M.; Gupta, S.; Gupta, T.; Raghav, A.; Singh, A., A review on recent advances and applications of nanofluids in plate heat exchanger. *Materials Today: Proceedings*. **2021**, *44*, 229-241, DOI: 10.1016/j.matpr.2020.09.460.

[2] Nakicenovic, N.; Nordhaus, W., Editors' introduction: The economics of technologies to combat global warming. *Energy. Econ.* **2011** *33*, 565-571, DOI: 10.1016/j.eneco.2011.02.001.

[3] Goharshadi, E. K.; Ahmadzadeh, H.; Samiee, S.; Hadadian, M., Nanofluids for heat Transfer enhancement-a review. *Phys. Chem. Res.* **2013**, *1*, 1-33, DOI: 10.22036/pcr.2013.2791.

[4] Das, S. K.; Choi, S. U. S.; Choi & Patel Hrishikesh, E., Heat Transfer in Nanofluids-A Review. *Heat. Transf. Eng.* **2006**, 27 (10), 3-19, DOI: 10.1080/01457630600904593.

[5] Hafiz, M. A.; Hassan, A.; Hassan, L.; Hafiz, T. B. M.; Malik, A. N., Experimental investigation of convective heat transfer augmentation for car radiator using ZnO-water nanofluids. *Energy*. **2015**, *84*, 317-324,

DOI: 10.1016/j.energy.2015.02.103.

[6] Mintsa, H. A.; Roy, G.; Nguyen, C. T.; Doucet, D., New temperature dependent thermal conductivity data for water-based nanofluids, *Int. J. Therm. Sci*. **2009** ,*48*, 363-371, DOI: 10.1016/j.ijthermalsci.2008.03.009.

[7] Chandrasekar, M.; Suresh, S.; Chandra Bose, A., Experimental investigations and theoretical determination of thermal conductivity and viscosity of Al_2O_3/water nanofluid. *Exp. Therm. Fluid. Sci*. **2010**, *34*, 210-216, DOI: 10.1016/ j.expthermflusci.2009.10.022.

[8] Asleshirin, S.; Mazaheri, H.; Omidkhah Nasrin, M. R.; Hassani Joshaghani, A., Experimental investigation of the effect of Al_2O_3 nanoparticles with spherical and rod-

[9] shaped morphologies on the thermophysical properties of ionic nanofluids. *Scientia Iranica C*., **2021**, 28 (3), 1452-1463, DOI: 10.24200/sci.2021.55859.4435.

[10] Ren, Y.; Xie, H.; Cai, A., Effective thermal conductivity of nanofluids containing spherical nanoparticles. *Appl. Phys*. **2005**, 38, 3958-3961, DOI: 10.1088/0022-3727/38/21/019.

[11] Chavan, D.; Pise, A., Experimental Investigation of Effective Viscosity and Density of Nanofluids. *Materials Today: Proceedings*. **2019**, *16*, 504-515, DOI: 10.1016/j.matpr.2019.05.122.

[12] Abbasian Arani, A. A.; Dehghani Yazdeli, R., Effects of uncertainties of conductivity models on mixed convection for Al_2O_3 nanofluid. *Scientia. Iranica. B*., **2016**, *23* (3) 951-965, DOI: 10.24200/sci.2016.3864.

[13] Eastman, J. A.; Phillpot, S. R.; Choi, S. U. S.; Keblinski, P., Thermal transport in Nanofluids *Annual. Rev. Mater. Res*. **2004**, *34*, 219-246, DOI: 10.1146/ annurev.matsci.34.052803.090621.

[14] Buschmann, M. H.; Azizian, R.; Kempe, T.; Julia, J. E.; Martinez-Cuenca, R.; Sunden, B.; Wu, Z.; Ari Seppala, T. A., Correct interpretation of nanofluid convective heat transfer. *International Journal of Thermal Sciences.* **2018**, *129*, 504-531, DOI: 10.1016/ j.ijthermalsci.2017.11.003.

[15] Vishwas, V.; Vadekar, M., ILs as heat transfer uids - An assessment using industrial exchanger geometries. *Applied Thermal Engineering.* **2017**, *111* (25) 1581-1587, DOI: 10.1016/j.applthermaleng.2016.04.156.

[16] Choi, S. U. S., Nanofluids: from vision to reality through research. *J. Heat. Transfer.* **2009**, *131*, 033106-1-033106-9, DOI: 10.1115/1.3056479.

[17] Huminic, G.; Huminic, A., Application of nanofluids in heat exchangers: a review. *Renew. Sustain. Energy Rev*. **2012**, *16*, 5625-5638, DOI: 10.1016/j.rser.2012.05.023.

[18] Fan, X.; Chen, H.; Ding, Y.; Plucinski, P. K.; and Lapkin, A. A., Potential of 'nanofluids' to Further intensify microreactors. *Green. Chem*. **2008**, *10*, 670-677, DOI: 10.1039/b717943j.

[19] Peyghambarzadeh, S. M.; Hashemabadi, S. H.; Hoseini, S. M.; Seifi, J. M., Experimental study of heat transfer enhancement using water/ethylene glycol based nanofluids as a new coolant for car radiators. *Int. Commun. Heat. Mass. Transfer.* **2011**, *38*, 1283-1290, DOI: 10.1016/j.icheatmasstransfer.2011.07.001.

[20] Ganvir, R. B.; Walke, P. V.; and Kriplani., V. M. Heat transfer characteristics in nanofluid-A Review. *Renewable and Sustainable Energy Reviews*. **2017**, *75*, 451-460, DOI: 10.1016/j.rser.2016.11.010.

[21] Pordanjani, A. H.; Aghakhani, S.; Afrand, M.; Mahmoudi B.; Mahian, O.; Wongwises. S., An updated review on application of nanofluids in heat exchangers for saving energy. *Energy Conversion and Management*. **2019**, *198*, 111886, DOI: 10.1016/ j.enconman.2019.111886.

[22] Mohankumar, T.; Rajan, K.; Sivakumar, K.; Gopal. V., Experimental Analysis of Heat Transfer Characteristics of Heat Exchanger Using Nano Fluids. *Mater. Sci. Eng*. **2019**, *574*, 012011, DOI: 10.1088/1757-899X/574/1/012011.

[23] Yadav, D.; Nirala, A.; Kumar, R.; Singh. P. K., Density variation in nanofluids as a function of concentration and temperature. *Materials Today: Proceedings.* **2021**, *46* (15), 6576-6580, DOI: 10.1016/ j.matpr.2021.04.052.

[24] Deepak Selvakumar, R.; Wu, J., comprehensive model for effective density of nanofluids based on particle clustering and interfacial layer formation. *Journal of Molecular Liquids.* **2019**, *92*, 111415, DOI: 10.1016/j.molliq.2019.111415.

[25] Zendehasbagh, S.; Majdan-Cegincara, R.; Magnetorheological and Volumetric Properties of Starch and Polyethylene Glycol Solutions in the Presence of NiO Nanoparticles. *Phys. Chem. Res*.,

2017, *6* (1), 45-66, DOI: 10.22036/pcr.2017.92605.1399.

[26] Vajjha, R. S.; Das, D. K.; Mahagaonkar, B. M., Density measurement of different nanofluids and their comparison with theory. *Petrol. Sci. Technol*. **2009**, *27*, 612-624, DOI: 10.1080/10916460701857714.

[27] Pak, B. C.; Cho, Y. I., Hydrodynamic and heat transfer study of dispersed fluids with submicron metallic oxide particles. *Exp. Heat. Transfer*. **1998**, *11*, 151-170, DOI: 10.1080/08916159808946559.

[28] Pakravesh, A.; Zarei, H., On the Effect of the Hard-sphere Term on the Statistical Associating Fluid Theory Equation of State. *Phys. Chem. Res.* **2022**, *10* (1), 45-56, DOI: 10.22036/PCR.2021.291384.1928.

[29] Mousazadeh, M. H., An Improved ISM Equation of State for Polar Fluids. *Phys. Chem. Res.* **2019**, *7* (3), 467-474, DOI: 10.22036/pcr.2019.171467.1591.

[30] Hosseini, S. M., Application of Carnahan-Starling-vdW-β Equation of State for Refrigerant *Fluids. Phys. Chem. Res*. **2018**, *6* (2), 447-462, DOI: 10.22036/pcr.2018.116571.1458.

[31] Fadaei-Nobandegania, F.; Alavianmehr, M. M.; Mohsenipour, A. A.; Moghadasi, J.; Faghihi, M. A., VLE Properties from ISM Equation of State: Application to Pure and Mixture, *Phys. Chem. Res*., **2015**, *3* (1), 16-23. DOI: 10.22036/pcr.2015.7298.

[32] Sharafi, Z.; Hosseini, S. M.; Jahromi, L. D., Modified equation of state extended to imidazolium-, phosphonium-, pyridinium-, pyrrolidinium- and ammonium-based ionic liquids. *Ionics*. **2012**, *18*, 829-835, DOI: 10.1007/s11581-012-0687.

[33] Mozaffari, F.; Mousavi, S. M. R., PVT properties of imidazolium-, phosphonium-, pyridinium-pyrrolidinium-based ionic liquids using critical point constants. *Phys. Chem. Liq*., **2017**, *55*, 11-18, DOI: 10.1080/00319104.2016.1163557.

[34] Mozaffari, F., Modelling the volumetric properties of ionic liquids using a modified perturbed hard-sphere-chain equation of state. *Phys. Chem. Liq*. **2018**, *56*, 627-634, DOI: 10.1080/00319104.2017.1371303.

[35] Song, Y.; Lambert, S. M.; Prausnitz, J. M., A Perturbed Hard-Sphere-Chain Equation of State for Normal Fluids and Polymers. *Ind. Eng. Chem. Res*. **1994**, *33*, 1047-1057, DOI: 10.1021/ie00028a037.

[36] Eslami, H., A perturbed hard-sphere-chain equation of state for liquid metals. *Journal of Nuclear Materials*. **2005**, *336*, 135-139, DOI: 10.1016/j.jnucmat.2004.08.011.

[37] Carnahan, N. F.; Starling, K. E., Equation of state for nonattracting rigid spheres. *J. Chem. Phys*. **1969**, *51*, 635-636, DOI: 10.1063/1.1672048.

[38] Song, Y.; Lambert, S. M.; Prausnitz, J. M., Liquid-liquid phase diagrams for binary polymer solutions from a perturbed hard-sphere-chain equation of state. *Chem. Eng. Sci*. **1994**, *49*, 2765-2775, DOI: 10.1016/0009-2509(94)E0096-9.

[39] Sharafi, Z.; Eslami, H., A modified perturbed hard-sphere-chain equation of state for Liquid refrigerant mixtures. *Physics and Chemistry of Liquids*. **2013**, *51* (4), 507-516, DOI: 10.1080/00319104.2012.747202.

[40] Mansoori, G.; Carnahan, N.; Starling, K.; Leland, Jr. T., Equilibrium thermodynamic properties of the mixture of hard spheres. *J. Chem. Phys*. **1971**, *54*, 1523-1525, DOI: 10.1063/1.1675048.

[41] Cabaleiro, D.; Pastoriza-Gallego, M. J.; Gracia-Fernández C.; Piñeiro, M. M.; Lugo, L., Rheological and volumetric properties of TiO_2-ethylene glycol nanofluids. *Nanoscale. Res. Lett*. **2013** *8* (286), 1-13, DOI: 10.1186/1556-276X-8-286.

[42] Han, F.; Zhang, J.; Chen, G.; Wei, X., Density, viscosity, and excess properties for aqueous Poly (ethylene glycol) solutions from (298.15 to 323.15) K. *J. Chem. Eng. Data*., **2008**, 53, 2598-2601, DOI: 10.1021/JE800464T.

[43] Lemmon, E.; McLinden, M.; Friend, D., Thermophysical Properties of Fluid Systems in NIST Chemistry WebBook, NIST Standard Reference Database Number 69, Eds. Linstrom, PJ and Mallard, WG, National Institute of Standards and Technology, Gaithersburg MD, 20899. In webbook. nist. gov (accessed October 28, 2012), **2011**, DOI: 10.18434/T4D303.

[44] Ifeacho, P., Semi-conducting Metal Oxide Nanoparticles from a Low-pressure Premixed H_1tn2/O_1tn2/Ar Flame: Synthesis and Characterization. **2008**, *Cuvillier Verlag. Gottingen.* DOI: cuvillier.de/de/shop/publications/1275.

[45] Cabaleiro, D.; Pastoriza-Gallego, M.; Piñeiro, M.;

Lugo, L., Characterization and measurements of thermal conductivity, density and rheological properties of zinc oxide nanoparticles dispersed in (ethane-1,2-diol + water) mixture. *J. Chem. Thermodyn*. **2013**, *58*, 405-415, DOI: 10.1016/j.jct.2012.10.014.

[46] Mariano, A.; Pastoriza-Gallego, M. J.; Lugo, L.; Mussari, L.; Piñeiro, M. M., Co_3O_4 ethylene glycol-based nanofluids: thermal conductivity, viscosity and high pressure density. *Int. J. Heat. Mass. Transf.* **2015**, *85*, 54-60, DOI: 10.1016/ j.ijheatmasstransfer. 2015.01.061.

[47] Pastoriza-Gallego, M.; Casanova, C.; Legido, J.; Piñeiro, M., CuO in water nanofluid: influence of particle size and polydispersity on volumetric behavior and viscosity. *Fluid. Phase. Equilib*. **2011**, *300*, 188-196, DOI: 10.1016/j.fluid.2010.10.015.

[48] Zafarani-Moattar, M. T.; Majdan-Cegincara, R., Effect of temperature on volumetric and transport properties of nanofluids containing ZnO nanoparticles poly (ethylene glycol) and Water. *J. Chem. Thermodyn*. **2012**, *54*, 55-67, DOI: 10.1016/j.jct.2012.03.010.

[49] Mariano, A.; Pastoriza-Gallego, M. J.; Lugo, L.; Camacho, A.; Canzonieri, S.; Piñeiro, M. M., Thermal conductivity, rheological behaviour and density of non-Newtonian ethylene glycol-based SnO_2 nanofluids. *Fluid. Phase. Equilibria.* **2013**, *337*, 119-124, DOI: 10.1016/j.fluid.2012.09.029.